A Computer-Vision Based Apparatus For The Measurement of Planar Movement : An Application in physiotherapy.

Donald Boivin[1],Denis Laurendeau[1], François Comeau[2] & Carol Richards[2]

[1]Laboratoire de vision et systèmes numériques
Département de Génie Electrique
Université Laval, Québec
Canada, G1K 7P4

[2]Centre de recherche en neurobiologie
Hôpital de l'Enfant-Jésus
Québec, Canada
G1J 1Z4

Abstract

The purpose of this paper is to present a computer vision-based apparatus designed for gait analysis of subjects. Under control of a host computer, the system digitizes a standard video signal and extracts the center of gravity of several markers placed on the subject's lower limbs (leg, knee, ankle, foot). It computes the distance between markers in "world coordinates" for all sampled image frames. The markers' space coordinate vs time data are useful to the physiotherapist who can use them to compute various motion parameters of the subject's limbs such as displacement, speed and acceleration. The error made on the measurements is less than 5 % for displacements of 5 cm with the camera 4 meters away from the patient. The main contribution of this work is to provide a low-cost yet easy to use and flexible motion data acquisition apparatus for clinical research in physiotherapy. Furthermore, the architecture of the system permits easy interfacing with various host personal computers.

Résumé

Ce travail présente un appareil de vision par ordinateur conçu pour faciliter l'étude du mouvement de patients en physiothérapie. L'appareil, sous la commande d'un ordinateur hôte, numérise le signal provenant d'une caméra vidéo et calcule le centre de gravité de marqueurs réfléchissants placés sur les membres inférieurs (jambe, genou, cheville, pied) du sujet. Les coordonnées des marqueurs dans l'espace tridimensionnel en fonction du temps sont ensuite calculées en utilisant les centres de gravité trouvés précédemment et en se basant sur la géométrie du système. La connaissance de l'évolution temporelle de ces coordonnées spatiales est utile au physiothérapeute qui peut calculer des paramètres objectifs d'analyse du mouvement tels le déplacement, la vitesse et l'accélération des parties de membre associées au marqueurs. Les coordonnées spatiales calculées par l'appareil montrent une précision de 5% sur des déplacements de 5 cm lorsque les marqueurs réfléchissants sont placés à une distance de travail de 4 m. Le principal apport de ce travail est qu'il fournit au physiothérapeute un outil flexible, peu coûteux et simple d'usage pour la recherche clinique. De plus, l'appareil dont il est question peut être interfacé facilement à plusieurs types d'ordinateurs personnels à un coût très raisonnable et sans subir de modifications majeures.

Keywords

Hardware implementation, motion analysis, biomedical application, moving light displays, vision in physiotherapy.

I- Introduction

Gait analysis is a wide research area in physiotherapy. A major problem in this field is the extraction of motion parameters such as the position of a patient's lower limbs during walk. The principal objectives of this project were to design a low-cost yet easy-to-use and flexible gait analysis system based on video information that could be interfaced to a standard microcomputer. A premium requirement was that the system should not interfere with other sensors already interfaced to the microcomputer (force plate, electrodes, etc).

The physiotherapy literature reveals that goniometers [1-5] (which give angles between segments), force plates (measuring force applied to the ground) and electromyographic signals (monitoring muscular electrical activity) are commonly used in such analysis. However, the problem with these devices is that they give no explicit information on the position of the subject in space and time. A cine-camera [7-11] can be used to obtain spatio-temporal information on the subject but the extraction of meaningful parameters from the film and their combination with data from other sources is time consuming and prone to error since it is often done manually. More recent systems rely on a tv-camera and on video processing hardware [12-13] to extract the motion parameters in real-time. The camera looks at reflective markers placed on the subject's limbs. Some systems, dedicated to the motion analysis of athletes, use sophisticated and expensive hardware while others use an approach that requires a large video buffer memory and important video post-processing.

The computer vision literature proposes a wide range of approaches for motion analysis such as optical flow techniques [14-15] and range from stereo [16]. For an overview of several techniques for range acquisition, see [17]. The extraction of range from texture [18] and motion from texture changes vs time is also of interest. Despite their wide use in general computer vision problems, these approaches require, in most cases, a large amount of processing time and powerful computer resources (see [16] for stereo vision and [19]-[21] for texture analysis). For these reasons, they are not suitable for the present clinical application in physiotherapy.

A paper by Roach *et al.* [22] addresses the problem of determining the general 3D movement (translation and rotation) of an object from a sequence of images. However, the assumption is made that the images are pre-segmented and that the same set of feature points on the object is available in each image of the sequence.

The work of Raschid [23] on moving light displays (MLD) presents the perceptual aspects of the interpretation of motion by humans when the subjects are shown a set of moving light markers of objects against a stationary background. The problem of MLD interpretation is decomposed into three principal tasks: *i)* the search for correspondence between light

displays in successive frames, *ii)* the separation of the different objects in each frame and *iii)* the determination of subparts of the objects separated at step *ii)*. The light displays are not obtained from a real scene but are rather created by a program for the simulation of human walking movement [24]. The primary concern of the paper is the interpretation of the MLDs, the problem of estimating of the 3D coordinates of the light displays is not addressed. It is stated in the paper that the method of analysis is able to cope with occlusion between markers even though no attempt was made to test the system with occluded MLDs.

This work describes the hardware-software implementation details of a computer-vision based system for motion analysis in physiotherapy. This system is a compromise between very expensive video processing hardware and large video buffer systems. The main purpose of the system is to track reflective markers (similar to Rachid's MLDs) in space and compute their 3D coordinates in the sagittal plane (i.e. parallel to the image plane of the observer) at periodic time intervals. The system, based on a video camera, samples a standard video signal at a rate of up to 60 fields/s and extracts, in a few seconds and with good accuracy, the position of several reflective markers that are attached to the subject's lower limbs. The system is interfaced to a microcomputer and allows the combination of the motion information thus obtained with data from other sources (electromyographic and force signals, etc) that are already in use.

The paper is divided as follows. Section II discusses the system in general and describes the acquisition setup and geometrical considerations for the extraction of the 3D coordinates of the markers. Section III presents the architecture of the system as well as the various modes of operation. Section IV covers the software running in the microcomputer and in the system while section V discusses the accuracy, error analysis and overall performance of the system.

II- General Description of the System.

As shown in Fig II.1, the camera is mounted on a cart that travels in a direction parallel to the walking plane (sagittal plane). Reflective markers are placed on the subject's lower limbs (foot, ankle, knee, leg) as well as on the wall behind. Wall markers (also called background markers) and subject markers have a different area and wall markers are placed much higher than the subject markers for easy identification. During a run, the cart is moving at approximately the same speed as the subject. The background markers are disposed in such a way that at least three markers are included in the field of view of the camera during the run. This helps to reduce the occurences where the patient masks the background marker. With adequate lighting, the system is able to extract the information on the markers only, provided that they are significantly brighter than the rest of the scene. With the reflective markers on the wall and those placed on anatomical landmarks of the subject, it is possible to evaluate the movement of the limbs in the sagittal walking plane.

Fig. II.2 is a top view of the acquisition setup. The image plane is shown as the X-Z plane of the global reference frame (Z-axis being normal to the page) while distances between the camera and the walking plane or the background plane are shown on the Y axis. The distances measured on the image plane are marked with a prime. The distance D_1 is the distance between the image plane and the walking plane while D_2 is the distance between the walking plane and the background plane.

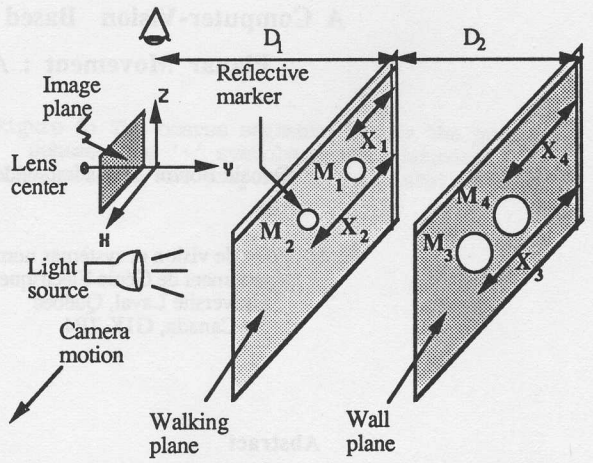

Fig. II.1 Side view of the measuring setup. Note that the three planes (walking, image and wall) are assumed parallel

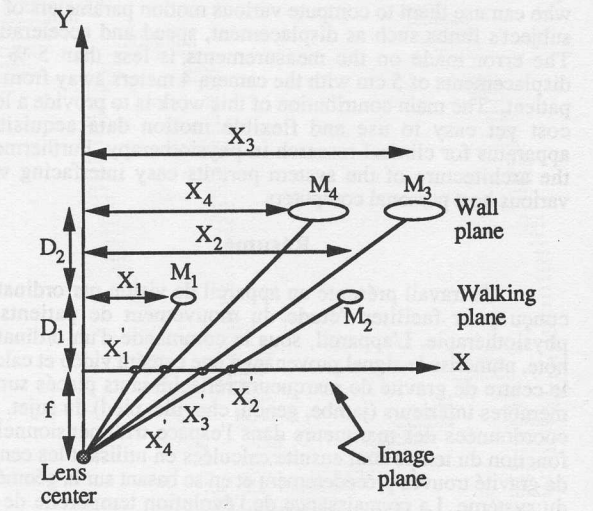

Fig. II.2 Geometry for parallax correction and Δx extraction (see eqs. (5), (6) and (7)). Top view of the scene in Fig. II.1.

From the geometry of Fig II.2, we can write Eqs. (1) through (7) below.

$$\frac{X_1}{[D_1+f\,]} = \frac{X'_1}{f} \qquad (1)$$

$$\frac{X_2}{[D_1+f\,]} = \frac{X'_2}{f} \qquad (2)$$

$$\frac{X_3}{[D_1+D_2+f\,]} = \frac{X'_3}{f} \qquad (3)$$

$$\frac{X_4}{[D_1+D_2+f\,]} = \frac{X'_4}{f} \qquad (4)$$

$$[X_2 - X_1] = \frac{[D_1+f\,]}{f} * [X'_2 - X'_1] \qquad (5)$$

$$[X_4 - X_3] = \frac{[D_1+D_2+f\,]}{f} * [X'_4 - X'_3] \qquad (6)$$

$$[X_3 - X_1] = \frac{[D_1+f\,]}{f} * [X'_3 - X'_1] + \frac{D_2}{f} * X'_3 \qquad (7)$$

Equations (1) and (2) express the perspective projection on the image plane of markers in the walking plane while equations (3) and (4) express the perspective projection on the image plane of markers in the background plane. Equation (5) shows that the relative position between markers 1 and 2 in the walking plane is proportional to their relative distance on the image plane. A similar expression holds for markers 3 and 4 in the background plane (Eq. (6)). With *a priori* knowledge of the distances between markers 1-2 and 3-4 in a calibration run performed with a special template (see [25] for details on the least-squares fit calibration procedure), the proportionality constants in Eqs. (5) and (6) can be computed easily and the relative distance between each marker in the walking plane and a background marker can be obtained from Eq. (7). This means that, in a normal run, if at least one background marker is visible in each video field (e.g. is not masked by the patient), the position of markers on the subject's limbs can be obtained relative to that background marker. Finally, similar equations may be obtained for the vertical (Z) axis on the image plane.

III- Architecture of the Sytem.

The main purpose of the system is to detect the presence of the reflective markers in the walking plane and in the background plane in each field of the video image obtained from the camera and then compute the position of the center of gravity (COG) of each marker. The values for the COG are replaced in Eq. (7) and the position of the markers in the walking plane are computed easily. To achieve the detection of the COGs, the system is comprised of three principal modules: *i)* the analog to digital video conversion circuit (A/DVC), *ii)* the digital image processing and control circuit (DIPCC) and *iii)* the parallel interface circuit (PIC).

The global architecture of the system is depicted in Fig III.1. The video sampling system is interfaced to a host microcomputer (in this case an IBM PC-AT) through a parallel communication interface. The host can program the system's operating parameters and has access to the motion analysis information through this interface. The host is also used for data storage on disk and graphical representation of the results.

The A/DVC module takes the incoming analog video signal from the camera (or VCR) and converts it to a binary signal. The digital signal is set to logic '1' if the analog signal is greater than a given threshold and it is set to '0' otherwise. A one bit conversion has been adopted to minimize the size of the image memory and reduce the cost of the digitizing hardware. For flexibility, the threshold level, the X and Y resolution of the sampled image and the rate of image sampling (number of fields per second that are considered) are programmable. There are 128 different threshold levels combined with an analog fine gain tuning. Three different image resolutions are available: 256 x 240, 128 x 120 and 64 x 60. There are also three different image sampling rates: 60 fields/s, 30 fields/s and 15 fields/s.

The main components of the DIPCC are: *i)* an 8 bit microprocessor (INTEL 8088) which receives and interprets the instructions from the host, computes the COG and controls the various functions of the system, *ii)* a bank of read only memory (ROM), *iii)* several groups of random access memory (RAM), and *iv)* control logic. The (ROM) is 16 Kbytes deep and contains the program that is executed by the microprocessor. The RAM is divided in two different parts. The first part (RAM#0, 32Kbytes) is reserved for program variables. The second part is divided in three banks of 32K each. These banks contain the data describing the images. It is important to choose a compact data representation for the digitized video signal for two reasons: first, a good representation requires less memory for storage and second, it allows a fast computation of the COG of each marker.

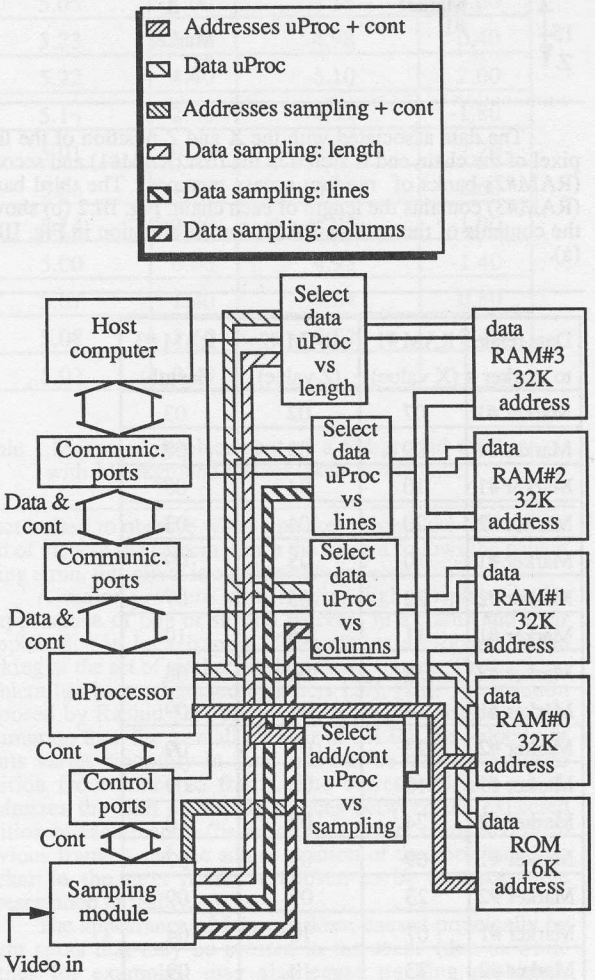

Fig. III.1 Block diagram of the system

The chain code representation [26] was chosen to encode the binary information of the digitized image. Let us assume the situation in Fig. III.2 (a) which shows several video lines of the same field with pixels belonging to two different markers. If we make the hypothesis that the markers will always yield uniform white blobs in the image plane, it is possible to encode a series

of white dots on a scanning line by specifying the length of the series and the image coordinates of its end point.

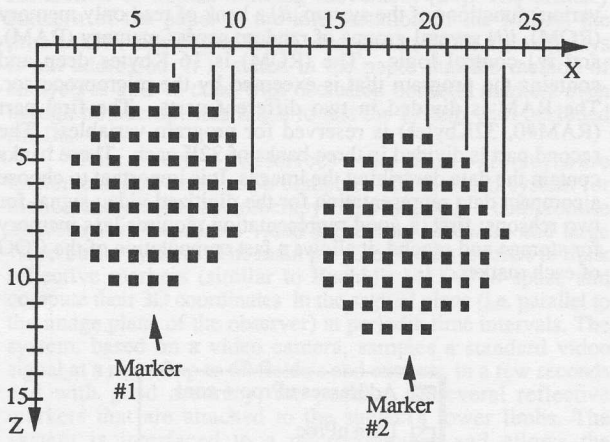

The data associated with the X and Z position of the last pixel of the chain end is stored in the first (RAM#1) and second (RAM#2) banks of random access memory. The third bank (RAM#3) contains the length of each chain. Fig. III.2 (b) shows the contents of the various RAMs for the situation in Fig. III.2 (a).

Data related to marker #	RAM #1 (X value)	RAM #2 (Z value)	RAM #3 (length)
Marker #1	07	02	03
Marker #1	09	03	07
Marker #1	10	04	08
Marker #2	20	04	03
Marker #1	10	05	09
Marker #2	22	05	07
Marker #1	11	06	10
Marker #2	23	06	08
Marker #1	10	07	09
Marker #2	23	07	09
Marker #1	10	08	09
Marker #2	24	08	10
Marker #1	09	09	07
Marker #2	23	09	09
Marker #1	07	10	04
Marker #2	23	10	09
Marker #2	22	11	07
Marker #2	20	12	04

Fig III.2(b) Representation of chain code in memory. Chains of Fig. III.2 (a)

The construction and recording of the chain codes is performed in real-time on successive fields of a run. At the end of a run, the memory banks are filled with the chain codes of the various markers (subject and background) and the field number from which they were extracted. A chain-code analysis program in ROM may then reconstruct the various markers from their chain-code and compute the COGs of the markers in each field.

A typical sequence of operations is as follows: the host sends a "start sampling" command to the system with the chosen resolution (image size and number of fields/sec) and threshold. Then, the microprocessor interprets the command, releases the bus and enters a halt state. The bus is taken over by the A/DVC module which digitizes the video signal, builds the chain codes and stores the information simultaneously in the appropriate memory banks. Once the sampling run is over, the A/DVC module relinquishes the bus to the microprocessor which can access the memory banks, reconstruct the markers and compute the coordinates of the COGs. The host can then read the coordinates of the COGs from the system and compute the coordinates of the markers in the walking plane once the background markers have been identified. In this implementation, the background markers have a larger area than the walking plane markers. The area of a marker may be recovered at the marker reconstruction operation by simply adding the sizes of the chain-codes associated with it.

The architecture described above allows a fast image sampling rate (5 MHz) without using much RAM. Fig III.2 (a) and (b) allows the comparison between memory requirements for chain-code sampling and standard coordinates sampling. For chain-code sampling (Fig III.2 (b)), it takes 54 memory cells to store the information contained in Fig III.2 (a). With a standard image representation (and no data compression), it would take two cells (for the X and Z coordinates) for each dot in the image and Fig III.2 (a) would require 264 memory cells. Chain-code sampling may also be compared more realistically with the familiar bitmap sampling used in many computer vision applications. For a scene containing 6 subject markers (approx. 10X10 pixels by marker) and 3 background markers (approx. 20X20 pixels by marker) and assuming a full resolution of 256X256 pixel/frame and a maximum number of frames of 256, the memory requirements for the chain-code sampling would be:

$$\left(20\frac{chains}{back} * 3back + 10\frac{chains}{subj} * 6subj\right) * 3\frac{bytes}{chain} * 256frames * \frac{1}{1024} = 90Kbytes$$

For the same number of markers at the same resolution and the same number of frames, the bitmap sampling would require:

$$\left(256 * 256\frac{pixels}{frame}\right) * \frac{1}{8}\frac{byte}{pixels} * 256frames * \frac{1}{1024} * \frac{1}{1024} = 2Mbytes$$

The required memory for chain-code sampling is thus 20 times smaller than for bitmap sampling. The amount of memory that is required by chain-code sampling increases with the number of markers. Finally, the chain-code representation has the advantage of performing part of the segmentation of the MLD scene by automatically grouping into chains successive pixels on the same video line.

IV- Software

The system software is composed of two main programs. The first one, a menu-driven program written in C, runs on the host computer. The major function of this program is to communicate with the video system. It can send the sampling parameters (such as image resolution, time sampling resolution, threshold for image binarization, number of fields) and the control words ("reset", "start sampling", "calibrate", "compute COGs", "transfer data") to the system or receive data

and status ("COG coordinate data or chain-code data") from the system through the parallel communication interface. The program handles long term data storage and graphic data representation. It also computes the space coordinates of the markers by using Equation (7), the COGs in image coordinates computed by the system, and the calibration parameters obtained from a calibration run.

The second program, also written in C and stored in ROM, runs on the video system. It handles the communications with the host through the PCI. It receives, interprets and executes the commands from the host and controls the various modes of operation. The program also performs a memory test after each reset command from the host. Finally, it handles a preliminary reconstruction of the markers and the computation of the image coordinates of the COGs of the reconstructed markers. The original chain-code data stored in RAM banks #1 through #3 is also available to the host from this program. Since it is written in C, the program can be modified easily.

V- Experimental Results. Accuracy of the Method.

Table I summarizes the measurements made on a set of markers and compares the computed marker coordinates with their actual value. This experiment estimates displacement of a foreground marker with a background marker taken as reference. Between each sample, the foreground marker is moved to the right 5 cm along the x axis while the background marker is stationary. A Δx between the foreground and background markers is computed for each sample. The displacement of the foreground marker is then evaluated by differentiation of two successive Δx's. A sampling run of one field was programmed for each position measurement.

Displacements of 5 cm were chosen because they are representative of the displacements that are likely to occur in a typical gait experiment. As shown in Table 1, the accuracy obtained is satisfactory (± 5% error). Tests performed on walking patients confirmed this figure. The various sources of error are discussed below.

The accuracy of the computed coordinates for the markers in the walking plane depends on many factors. Some are related to the intrinsic limitations of the system (like image resolution in space and time) while others are related to the various components forming the system (lens, temperature ratings, marker size, etc). For the experiments, the camera was placed at a distance (D_1) of 3.6 m from the patient. The distance (D_2) between the patient and the background plane was 1 m. With a 16 mm lens mounted on the camera, the patient could be seen from head to toes (field of view approx. = 1.8 m). The image resolution was 240 X 256. It was observed that for such a lens and working distance, barrel-type lens distorsion was slightly noticeable. However, these aberrations were small enough as to be negligible (see [25] for details).

Marker size has a significant effect on accuracy [6]. The error made on the position of the COG of a large marker is much smaller than for a small one because of the digital nature of the image. Therefore the marker size must be chosen to minimize the error without being inconvenient for the patient. For this experiment, circular white paper markers with a diameter of 6 cm were used.

Light source orientation also has a very important effect on accuracy since it is responsible for the brightness of the markers in the image. If the source is misoriented, it will affect the shape and size of the image of the markers and by the same token, the position of the COGs. In the implementation of the system, the source is moved with the camera to reduce this effect and all other light sources are turned off during a run. A change in the orientation of the markers during a run (possibly caused by a twisting of the patient's leg or foot) can cause a similar error by altering the shape of the image of the marker. This effect is easy to observe when a marker reaches the limit of the field of view of the camera. Since the camera follows the patient during a run, this effect is considerably reduced.

Measured values Δx in cm	error %	Measured values Δx in cm	error %
4.99	-0.20	4.88	-2.40
4.91	-1.80	4.92	-1.60
5.07	1.40	5.05	1.00
5.03	0.60	4.90	-2.00
5.09	1.80	5.05	1.00
4.89	-2.20	4.99	-0.20
5.17	3.40	5.11	2.20
4.94	-1.20	5.00	0.00
5.05	1.00	5.15	3.00
5.23	4.60	4.98	-0.40
5.22	4.40	5.10	2.00
5.14	2.80	4.91	-1.80
5.01	0.20	4.89	-2.20
5.06	1.20	4.87	-2.60
5.14	2.80	4.95	-1.00
5.00	0.00	4.93	-1.40
5.07	1.40	5.04	0.80
5.08	1.60	5.02	0.40
5.02	0.40		

Table 1.Measured displacement of a foreground marker with a background marker taken as reference.

A major problem with moving light displays is the disappearance of one or several markers in a frame and their reappearance in later frames. This causes a problem in the tracking of the set of markers in successive frames. The tracking problem has been addressed by others [27], [28]. The solution proposed by Rachid [28] for marker tracking is based on the assumption that, for a small number of MLDs, the velocity of points varies smoothly in time and can be used to estimate position from frame to frame. The correspondence which minimizes the sum of the differences between the expected position of each marker (based on its velocity computed from previous frames) and the actual position of the corresponding marker in the next frame is chosen to be an acceptable representation of reality.

The appearance of false markers, caused principally by bright spots that may be present in the scene (due to white clothes for example), may also cause tracking problems. However, during the tests, this problem did not occur, even when the markers were placed on one subject's white shirt.

Equations (1)-(7), for the computation of the 3D coordinates of the markers in the sagittal plane from the position of their COG in the image, were established under the assumption that the patient moves in a plane parallel to the image plane of the camera. In practice, however, a patient rarely moves at a constant distance from the image plane. To see the effect of a difference between the trajectory of the patient and the

parameters obtained from the calibration run, let us consider the geometry in Fig. V.1 which shows a background marker M_3 and a subject marker M_1.

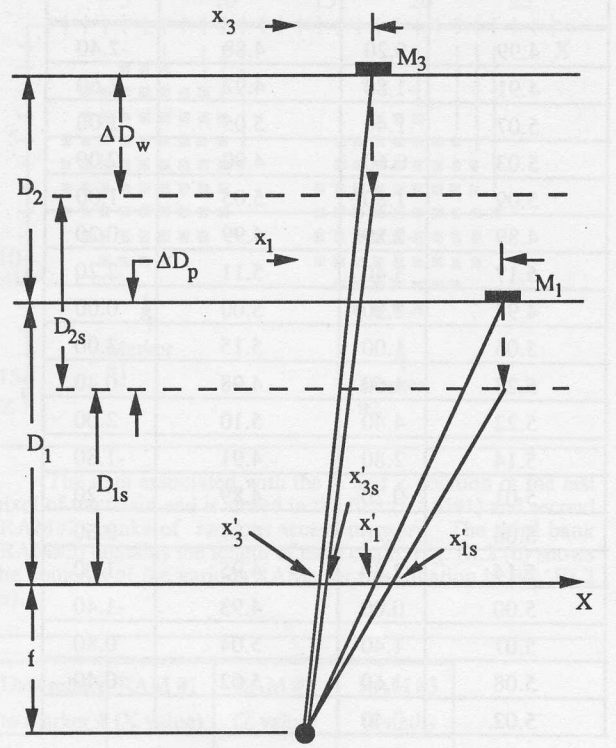

Fig. V.1 Geometry for error analysis.

During the calibration run, the marker M_1 was at a distance D_1 from the image plane and the marker M_3 was at a distance D_2 from the plane supporting M_1. The coefficients in Eq. (7) were obtained from this calibration run. Now during a normal run, the patient may move away from the plane at D_1 and the camera may move away from the background plane at D_2 (which is shown here as a displacement of the background marker from the plane at D_2). Therefore, the markers M_1 and M_3 are displaced by ΔD_p and ΔD_w from their value in the calibration run. Both ΔD_p and ΔD_w are signed values. From the geometry in the Fig. V.1, where ΔD_p and ΔD_w are greatly exagerated, we can write:

$$D_{1s} = D_1 - \Delta D_p \tag{8}$$

$$D_{2s} = D_2 - \Delta D_w + \Delta D_p \tag{9}$$

The coordinates of the images of M_1 and M_3 on the image plane are now x'_{1s} and x'_{3s}. These values are replaced in Eq. (7) to obtain the relative distance $[x_3\text{-}x_1]_s$ between M_1 and M_3:

$$[x_3 - x_1]_s = \frac{D_1 + f}{f}[x'_{3s} - x'_{1s}] + \frac{D_2}{f}x'_{3s} \tag{10}$$

From Fig. V.2 which shows an enlarged portion of Fig. V.1, we can write for x'_{1s} and x'_{3s} (see Appendix 1 for details):

$$x'_{1s} = x'_1 + \frac{\tan(\alpha_1) f\ \Delta D_p}{D_1 + f - \Delta D_p} \tag{11}$$

$$x'_{3s} = x'_3 + \frac{\tan(\alpha_3) f\ \Delta D_w}{D_1 + D_2 + f - \Delta D_w} \tag{12}$$

with

$$\tan(\alpha_1) = \frac{x_1}{D_1 + f} \tag{13}$$

$$\tan(\alpha_3) = \frac{x_3}{D_1 + D_2 + f} \tag{14}$$

Replacing (11)-(14) in (10) yields

$$[x_3 - x_1]_s = [x_3 - x_1] + \frac{\Delta D_w}{D_1 + D_2 + f - \Delta D_w} x_3 - \frac{\Delta D_p}{D_1 + f - \Delta D_p} x_1 \tag{15}$$

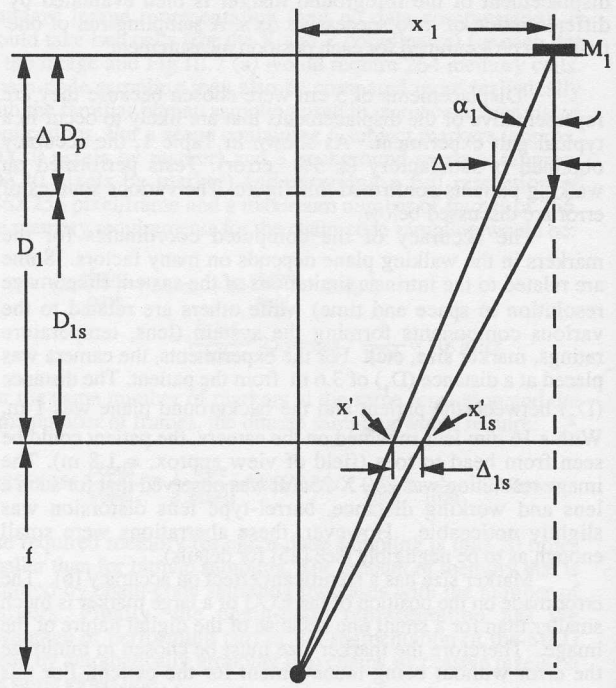

Fig. V.2 Geometry for the derivation of Eq. (11)

Making the assumption that ΔD_p and ΔD_w are much smaller than D_1+D_2, the last two terms in (15) may be written:

$$\frac{\Delta D_w}{D_1 + D_2 + f - \Delta D_w} \approx \frac{\Delta D_w}{D_1 + D_2 + f} \tag{16}$$

$$\frac{\Delta D_p}{D_1+f-\Delta D_p} \approx \frac{\Delta D_p}{D_1+f} \qquad (17)$$

With (16) and (17) in (15), the expression for the relative distance between M_1 and M_3 is given by:

$$[x_{3s}-x_{1s}] \approx [x_3-x_1] + \frac{\Delta D_w}{D_1+D_2+f}x_3 - \frac{\Delta D_p}{D_1+f}x_1 \qquad (18)$$

The error ε between the computed value $[x_3\text{-}x_1]_S$ and the actual value $[x_3\text{-}x_1]$ is simply:

$$\varepsilon \approx \frac{\Delta D_w}{D_1+D_2+f}x_3 - \frac{\Delta D_p}{D_1+f}x_1 \qquad (19)$$

Eq. (19) shows that the error ε is proportional to ΔD_w and ΔD_p. It is also proportional to x_1 and x_3, the coordinates of the markers in the reference frame of the camera. As stated above, $D_1 \approx 4$ m, $D_2 \approx 1$ m, and the field of view is approximately 2 m. Since the camera moves with the patient, marker M_1 remains in the field of view as does one of the background markers M_3 (-1 m < x_1, x_3 < 1 m). Fig. V.3 shows the evolution of the error ε as x_1 varies from -1m to +1m for a given value of x_3 between -1m and 1m and for $\Delta D_p = \Delta D_w = +0.02$ m which are typical values for trajectory variations. The largest absolute error ε occurs when the background marker M_3 is at one end of the field of view and marker M_1 is at the other end of the field of view. In this particular situation, the absolute error ε is 0.9 cm but the relative error is 0.5%. This situation should not occur very often since the camera moves with the patient and the subject markers are thus almost always located near the center of the field of view. Identical values of 0.02 m were chosen for ΔD_p and ΔD_w. However, the actual value for ΔD_w is smaller since the camera supporting cart is fixed to a rail parallel to the background wall.

Error caused by the variation of the patient-camera and background-camera distances (ΔDp=ΔDw=2cm)

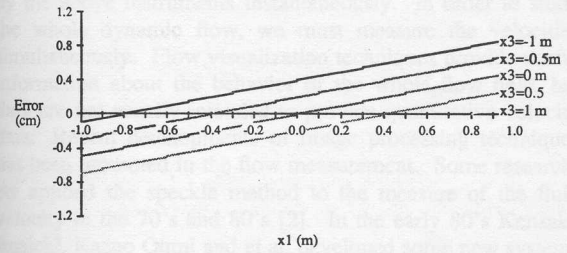

Fig. V.3 Results of error analysis.

VI. Conclusion

The system described above is a good compromise between highly sophisticated expensive systems and manual processing. Low cost, reliability, good accuracy, high speed, ease of operation and calibration are all qualities making the system very attractive. The fact that the system can be easily adapted to various host computers and programmed for specified modes of operation makes it very versatile. Finally, the menu driven software makes it easy to operate for non-specialised users. The system was primarily designed as a visual input device for clinical research in physiotherapy and recent tests have shown that the system performs well at this task.

VII. Appendix 1

The different steps leading to Eqs. (11) and (12) are presented in this section.

From Fig. V.2 and marker M_1:

$$x'_{1s} = x'_1 + \Delta'_{1s} \qquad (20)$$

and

$$\tan(\alpha_1) = \frac{\Delta}{\Delta D_p} = \frac{x_1}{D_1+f} \qquad (21)$$

From similar triangles,

$$\frac{\Delta'_{1s}}{\Delta} = \frac{f}{D_{1s}+f} \qquad (22)$$

With (21) and (8) in (22)

$$\Delta'_{1s} = \frac{f\,\Delta D_p}{D_1+f-\Delta D_p}\tan(\alpha_1) \qquad (23)$$

Replacing (23) in (20) we obtain Eq. (11). A similar procedure may be followed for marker M_3 and Eq. (12).

VIII. Acknowledgements

The authors would like to thank Mr. J. Ahern and Mr. C. Scaffidi for reading the manuscript and the reviewers for their helpful comments on ways of improving it. This work was supported in part by grant A4052 of the National Research Council of Canada.

IX. References.

[1] Johnson, R.C., Smidt, G.L. "Measurement of hip joint motion during walking: evaluation of an electrogoniometric method". *J. Bone Joint Surg.*, **51**, 1083-1094 (1969)

[2] Lamoreux, L.W. "Experimental kinematics of human walking." Ph.D. Thesis, Univ. California. (1970)

[3] Kettlekamp, D.B. "An electrogoniometric study of knee motion in normal gait". *J. Bone Joint Surg.*, **52A**, 775-790 (1970)

[4] Tipton, C.M., Karpovich, P.V. "Electrogoniometric records of knee and ankle movements in pathologic gait". *Arch. Phys. Med,* **46**, 267-272, (1965)

[5] Finley, F.R., Karpovich, P.V. "Electrogoniometric analysis of normal and pathological gaits". *Res. Quart. (Supplement)*, **35**, 379-384, (1964)

[6] Winter, D.A., Hobson, D.A., Greenlaw, R.K. "A microswitch shoe for use in locomotion studies". *J. Biomechanics*, **5**, 553-554, (1972)
[7] Marey, E.J. "Physiologie. Les applications de la chronophotographie à la physiologie expérimentale". *Rev. Sci.*, **51**, 321-327,(1983).
[8] Eberhart, H.D., Inman, V.T. "An evaluation of experimental procedures used in a fundamental study of human locomotion". *Annals N.Y. Acad Sci.*, **51**, 1213-23, (1951)
[9] Murray, M.P., Drought, A.B., Kory, R.C. "Walking patterns of normal men". *Bone Joint Surg.*, **46-A**, 335-360, (1964)
[10] Paul, J.P. "Forces transmitted by joints in the human body". *Proc. Inst. Mech. Engn.*, **181**, 8-15, (1967)
[11] Liberson, W.T. "Biomechanics of gait: A method of study". *Arch. Phys. Med Rehab.*, **46**, 37-48, (1965)
[12] Waas, R. "A digital optical scanning system for kinematic analysis". Ph. D. Thesis, Case Western Reserve, (1969)
[13] Winter, D.A., Greenland, R.K., Hobson, D.A. "A clinical approach to the study of human locomotion". *Digest 3rd Cdn. Med. & Biol. Engng. Conf.*, Halifax, N.S., Sept., (Sept. 1970).
[14] Horn, B.K.P. "Robot Vision", McGraw-Hill, New York, 509p., 1986.
[15] Hildreth, E.C. "The Measurement of Visual Motion", Mit Press, Cambridge, Mass, 241p., 1983.
[16] Shirai, Y. "Three-Dimensional Computer Vision", Springer Verlag, New York, 297 p., 1989.
[17] Poussart, D, Laurendeau, D. "3D Sensing for Industrial Computer Vision", in "Advances in Computer Vision" Springer-Verlag, Jorge L. C. Sanz Ed, pp. 216-253, (to be published in 1989).

[18] Jarvis, R. A. "A Perspective on Range Finding Techniques for Computer Vision," *IEEE Trans. on PAMI*, vol. PAMI-5, no. 2, pp. 122-139, March 1983.
[19] Kender, J.R. "Shape from Texture", *Proc. 6th IJCAI*, Tokyo, pp. 475-480.
[20] Wong, A.K.C., Shen, H.C. "Search Effective Multiclass Texture Classification", PRIP '82, pp. 208-213.
[21] Riley, M. D. "The Representation of Image Texture", AI-TR-649, MIT Memo, 67p., Sept. 1981.
[22] Roach, J.W., Aggarwal, J.K. "Determining the Movement of Objects from a Sequence of Images", *IEEE Trans. on PAMI*, vol. PAMI-2, no. 6, Nov. 1980, pp. 554-562.
[23] Raschid, R.F. "Towards a System for the Interpretation of Moving Light Displays", *IEEE Trans. on PAMI*, vol PAMI-2, no. 6, Nov. 1980, pp. 574-581.
[24] Cutting, J.E. "A Program to Generate Synthetic Walkers as Dynamic Point-Light Displays", *Behavior Res. Methods and Instrumentation*, vol. 10, no. 1, pp. 91-94, 1978.
[25] Boivin, D. "Système d'acquisition et de traitement d'information vidéo en temps réel pour l'analyse du mouvement en physiothérapie", Master's thesis, Laval University, Québec, Canada, December 1988, (in French).
[26] Ballard, D.H., Brown, C.M. "Computer Vision", Prentice Hall, 523 p., 1982.
[27] Ullman, S. "The Interpretation of Structure from Motion", MIT Press, Cambridge, Mass, 1979.
[28] Raschid, R. "Lights: A System for the Interpretation of Moving Light Displays", Ph. D. Dissertation, University of Rochester, Rochester, NY, 1980.